Real-Time Tracking of Yb^{3+}, Tm^{3+} Doped $NaYF_4$ Nanoparticles in Living Cancer Cells

DOI: 10.17691/stm2018.10.1.07
Received November 16, 2017

© **A.B. Kostyuk,** Junior Researcher, Laboratory of Optical Theranostics, Institute of Biology and Biomedicine[1];
E.L. Guryev, PhD, Researcher, Laboratory of Optical Theranostics, Institute of Biology and Biomedicine[1];
A.D. Vorotnov, Laboratory Assistant, Laboratory of Optical Theranostics, Institute of Biology and Biomedicine[1];
L.M. Sencha, Laboratory Assistant, Laboratory of Optical Theranostics, Institute of Biology and Biomedicine[1];
N.N. Peskova, Junior Researcher, Laboratory of Optical Theranostics, Institute of Biology and Biomedicine[1];
E.A. Sokolova, PhD, Junior Researcher, Laboratory of Optical Theranostics, Institute of Biology and Biomedicine[1];
L. Liang, PhD, Researcher, Department of Physics and Astronomy[2];
V.A. Vodeneev, DSc, Head of the Department of Biophysics, Institute of Biology and Biomedicine[1];
I.V. Balalaeva, PhD, Associate Professor, Department of Biophysics, Institute of Biology and Biomedicine[1]; Senior Researcher, Laboratory of Nanotheranostics, Institute of Molecular Medicine[3];
A.V. Zvyagin, DSc, Leading Researcher, Laboratory of Optical Theranostics, Institute of Biology and Biomedicine[1]; Director of the Centre of Biomedical Engineering, Institute of Molecular Medicine[3]; Associate Professor, Head of the Optical Biomedical Imaging and Sensing Group, ARC Centre of Excellence for Nanoscale BioPhotonics (CNBP)[2]

[1]Lobachevsky State University of Nizhni Novgorod, 23 Prospekt Gagarina, Nizhny Novgorod, 603950, Russia;
[2]Macquarie University, Balaclava Road, North Ryde NSW, Sydney, 2109, Australia;
[3]I.M. Sechenov First Moscow State Medical University, 8/2 Trubetskaya St., Moscow, 119991, Russia

The aim of the study was to demonstrate the possibility of real-time tracking of polyethylenimine-coated $NaYF_4$:Yb,Tm upconversion nanoparticles (UCNPs) in living cancer cells using wide-field microscopy technique.

Materials and Methods. Human breast adenocarcinoma SK-BR-3 cells and Yb^{3+}, Tm^{3+} doped $NaYF_4$ nanoparticles with anti-Stokes photoluminescence were used in the study. The nanoparticles were visualized using wide-field microscope with excitation at 975 nm and signal detection in 420–842 spectral range. The analysis of the displacement of UCNPs was performed by fitting the point spread function of the photoluminescent spots corresponding to UCNP location by the Gaussian function, and calculation of mean square displacement.

Results. UCNPs were rapidly internalized by SK-BR-3 cells and retained in the cells for at least 12 h. Two types of the particles motion were registered: (i) isotropic random spatial fluctuations with relatively small amplitudes and low rate of displacement, and (ii) flick and directional movements with rates up to 1.2 μm/s and total displacement up to tens of microns. The registered types of motion can be attributed to diffusion in local area and intracellular transport of nanoparticles encapsulated in vesicles, respectively.

Conclusion. The demonstrated tracking of UCNPs in human breast adenocarcinoma cells showed that Yb^{3+}, Tm^{3+} doped $NaYF_4$ nanoparticles are an advanced agent for dynamic studies of intracellular processes. The implemented scheme for UCNPs tracking provides long-term observation with preservation of cell viability for at least several hours. In total, almost complete absence of cell autofluorescence and UCNPs photobleaching, low invasiveness, fast rate of image acquisition allow us to consider the proposed approach as useful for a variety of tasks in biomedical research.

Key words: upconversion nanoparticles; single-particle tracking; wide-field microscopy.

How to cite: Kostyuk A.B., Guryev E.L., Vorotnov A.D., Sencha L.M., Peskova N.N., Sokolova E.A., Liang L., Vodeneev V.A., Balalaeva I.V., Zvyagin A.V. Real-time tracking of Yb^{3+}, Tm^{3+} doped $NaYF_4$ nanoparticles in living cancer cells. Sovremennye tehnologii v medicine 2018; 10(1): 57, https://doi.org/10.17691/stm2018.10.1.07

Introduction

The study of molecular transport, underlying biological processes, is one of the actively developing fields of science. The modern technical equipment for visualization and tracking of single molecules labeled with fluorescent probes allows real-time detection, identification, and tracking of individual molecules in biological systems [1]. The specificity of tracking in biological systems causes improved criteria for fluorescent dyes. In particular, it is

Corresponding author: Alexey B. Kostyuk, e-mail: kostyukalexey@mail.ru

necessary to ensure the consistency of the photophysical properties of the dye throughout the experiment. Thus, an important parameter is photostability (or resistance to photobleaching), i.e. the ability to maintain the photoluminescence (PL) intensity during prolonged excitation.

Organic dyes and genetically encoded fluorescent proteins are prone to rapid photobleaching and are not suitable for long-term studies. In addition, single fluorophores emit a relatively low number of photons, and their PL spectrum (~400–700 nm) falls within the region of high absorption of biological tissue, making it difficult to detect them. Inorganic luminescent nanoparticles are an alternative to fluorescent probes and proteins. Among them, semiconductor quantum dots have got widespread use for single molecules tracking. The successful use of quantum dots in tracking systems [2] is caused by a number of their advantages such as the exceptional brightness due to a high quantum yield (up to 90%) [3, 4], high photostability and resistance to chemical degradation. These properties make it possible to use quantum dots in long-term *in vitro* imaging [5, 6]. On the other hand, the presence of a fraction of non-radiating dark particles [7], as well as photoblinking [8] and cytotoxicity [9] limit their usage for tracking.

Upconversion nanoparticles (UCNPs) have recently emerged as a new class of inorganic photoluminescent nanoparticles that can successfully replace quantum dots [10]. UCNPs effectively convert the energy of absorbed infrared photons (~975 nm) into visible and near-infrared radiation. Unique photophysical properties of UCNPs, such as programmable spectra and narrow PL peaks, significant depth of optical detection *in vivo* [11], resistance to photobleaching [12, 13] and low cytotoxicity [14, 15], have provided their wide use in various types of biomedical research [16, 17].

Variety of inorganic matrices can serve as a base for UCNPs with a large selection of doping elements [16, 18]. However, the fluoride matrix co-doped with ytterbium and erbium or thulium ions ($NaYF_4$:Yb,Er/Tm) has got the most common use due to the high efficiency of upconversion (energy conversion). Remarkable photostability of UCNPs and the noninvasiveness of near-infrared excitation provide long-term visualization of processes of interest. The possibility was shown to visualize intracellular migration of $NaYF_4$ nanoparticles co-doped with Yb^{3+} and Er^{3+} for 6 h of continuous image acquisition [19]. Also, the use of similar UCNPs for rapid and background-free 3D visualization of dynamic processes in living cells was demonstrated [20]. Excitation of UCNPs in the infrared range provides an absence of cell autofluorescence, which almost completely eliminates the background signal out of focus and, therefore, greatly simplifies the determination of the 3D coordinates of UCNPs localization.

The aim of the study was to demonstrate the possibility of real-time tracking of $NaYF_4$:Yb,Tm upconversion nanoparticles coated with polyethylenimine in living cancer cells using wide-field microscopy technique.

Materials and Methods

Nanoparticles. Hexagonal $NaYF_4$ nanocrystals containing 8 mol% Tm^{3+}, co-doped with 20 mol% Yb^{3+} [21] were used in the work. To achieve colloidal stability of $NaYF_4$:Yb,Tm UCNPs in aqueous solutions they were surface coated with polyethylenimine (UCNP-PEI) [14].

The transmission electron microscopy images were obtained using CM10 microscope (Philips, The Netherlands) with an accelerating voltage of 100 kV and a resolution of 5.0 Å for a point and 3.4 Å for a line.

Cells. The cell line SK-BR-3 (human breast adenocarcinoma, ATCC number HTB-30) was cultured in the McCoy's 5A growth medium with 10% (v/v) fetal calf serum (HyClone, USA) and 2 mM L-glutamine in 5% CO_2 at 37°C. For passaging the cells were carefully detached using Versen solution (PanEco, Russia).

Tracking of UCNP-PEI in SK-BR-3 cells. SK-BR-3 cells were seeded in 96-well plates (BD Falcon, USA) at the density of $1 \cdot 10^4$ cells per well and cultured for 24 h at 37°C in 5% CO_2. The growth medium was then replaced with PBS containing 5 μg/ml UCNP-PEI, and the cells were incubated for 2 h. After that, the UCNP-PEI solution was replaced with fresh growth medium, and the cells were incubated overnight.

Tracking of UCNP-PEI in SK-BR-3 cells was carried out using the home-built setup created on the basis of the Axio Observer A1 microscope (Carl Zeiss, Germany). The scheme of the setup is shown in Figure 1.

The exciting radiation is generated by a laser diode LDD-10 (Semiconductor devices, Russia) at 975 nm. Then, the laser diode emission is assembled into a multimode optical fiber (200 μm diameter) connected to a collimator F280SMA-980 (Thorlabs, USA), which forms a Gaussian beam with a diameter of 2 mm. Further, a uniform illumination of the sample is created using a lens focusing on the back focal plane of an immersion oil objective C Plan Apochromat 63× NA1.4 Oil (Carl Zeiss, Germany). On the way to the sample, the excitation radiation is spectrally filtered by a laser clean-up filter LD01-975/10 (Semrock, USA), after that the radiation is reflected from the dichroic mirror ZT1064rdc-sp (Chroma, USA) and focused on the sample using the objective. The PL from the sample passes through the objective, dichroic mirror, and two successively set edge short-pass filters FF01-842/SP (Semrock, USA), which cut off laser radiation and transmit the spectral range of the PL registration (420–842 nm). The image is captured through the side port of the microscope to the iXon3 897 EMCCD camera (Andor, UK).

The excitation of the samples was carried out in a continuous mode at 975 nm with a radiation intensity of 950 W/cm^2 and an image acquisition time of up to 30 min. Registration of epi-luminescence images was performed in a mode of continuous image acquisition (frame transfer kinetics) with a frequency of ~5 Hz and an exposure of each frame of 200 ms. Using a red LED, the sample was illuminated every 5 frames to obtain brightfield images

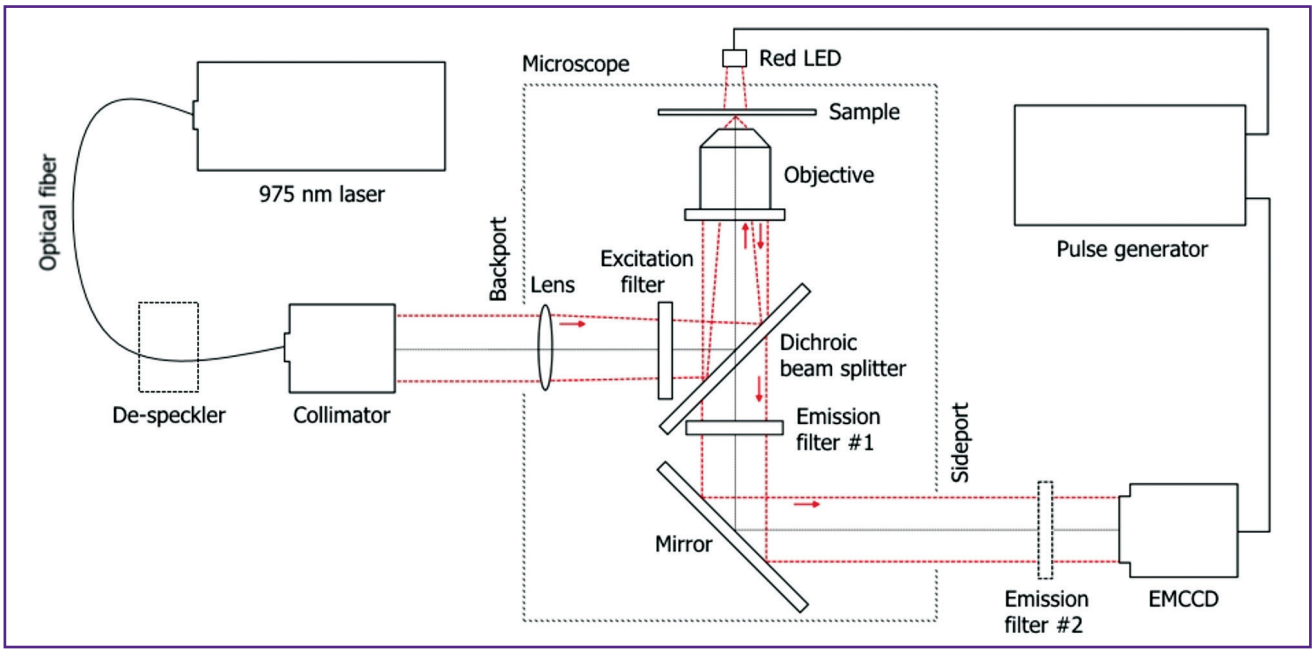

Figure 1. The scheme of the experimental setup for upconversion nanoparticles tracking in living cells
LED is the light-emitting diode, EMCCD is the electron multiplying charge coupled device

in which the location and morphology of the cells were determined. Synchronization of LED start was carried out by means of the pulse generator AKIP-3413/1 (Prist, Russia), which received a control signal from the iXon3 897 camera (Andor, UK). All images were acquired at room temperature.

Analysis of trajectories of UCNP-PEI. The PL signal of nanoparticles with a size below the diffraction limit is well described by the normal distribution. Therefore, to determine the coordinates of the UCNP-PEI location in cells, we fitted the diffraction spots corresponding to UCNP-PEI by the two-dimensional Gaussian function (G) [22]:

$$G(x,y)=I_0\cdot\exp\left[-\left(\frac{(x-x_0)}{2s_x^2}+\frac{(y-y_0)}{2s_y^2}\right)\right], \quad (1)$$

where x_0, y_0 is the center of the diffraction spot, $2\sqrt{2\ln 2}\cdot s_{x,y}$ is its full width at half maximum along the axis x and y, respectively and I_0 is the peak intensity.

To determine the transport speed and the type of motion of the marked objects, the mean square displacement (MSD) was calculated for each time point of the UCNP-PEI trajectory:

$$MSD(n\tau)=\frac{1}{N-n}\sum_{i=1}^{N-n}[(x_0[(i+n)\tau]-x_0(i\cdot\tau))^2+ +(y_0[(i+n)\tau]-y_0(i\cdot\tau))^2], \quad (2)$$

where τ is the acquisition time, N is the total number of frames, and n is the frame number in sequence.

The plot MSD($n\tau$) has characteristic features for each type of particle motion. The linear dependence of MSD on time with a slope of 4D, where D is diffusion coefficient, corresponds to an isotropic random motion. If there is an additional directional motion with a velocity v, MSD($n\tau$) is expressed as:

$$MSD(n\tau)=4Dn\tau+(\upsilon n\tau)^2. \quad (3)$$

In the case when the random motion of a particle is bounded by the region L, the graph MSD($n\tau$) is described by the following expression:

$$MSD(n\tau)=\frac{L^2}{3}\left[1-\exp\left(\frac{12Dn\tau}{L^2}\right)\right], \quad (4)$$

where L^2 is the confined area in which the diffusion is restricted.

Results and Discussion

According to the transmission electron microscopy data on the size distribution, $NaYF_4$:Yb,Tm UCNPs were monodisperse with an average nanocrystal size of 28.1±2.2 nm (Figure 2). This type of Tm^{3+}-doped UCNPs is characterized by PL emission with several main peaks in the visible (455 nm, 514 nm, and 660 nm) and near-infrared (744 nm, 782 nm, and 802 nm) spectral regions when excited at 980 nm [21].

Incubation of UCNP-PEI with SK-BR-3 cells for 2 h was accompanied by receptor-independent endocytosis. The internalized nanoparticles were retained in the cell for a long time (at least 12 h). We visualized the behavior of particles in the cell after this time period. Figure 3 shows images of UCNP-PEI in SK-BR-3 cell extracted from a video file recorded in real-time at a

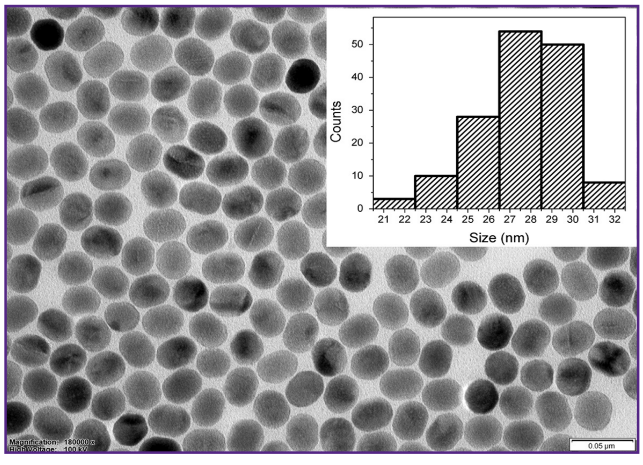

Figure 2. The transmission electron microscopy image of $NaYF_4$:Yb,Tm nanoparticles
On the insert, the size distribution of the nanoparticles

rate of 5 frames per second. Taking into account the size of UCNPs, which is about ~30 nm, the most likely mechanism of the nanoparticles uptake is pinocytosis, leading to encapsulation of particles in vesicular organelles such as endosomes and their subsequent intracellular transport [23, 24]. The positive surface charge of the PEI-coated UCNPs, presumably, leads to the electrostatic interaction with negatively charged membrane phospholipids, such as phosphatidylserine and phosphatidylglycerol, and facilitates the first steps of the internalization.

The proposed scheme for recording luminescence causes a selective signal acquisition only from UCNP-PEI (Figure 3, *middle row*). When exciting UCNPs by a continuous wave laser diode at 975 nm, the autofluorescence signal is undetectable [20]. The blurred PL signal is caused by UCNPs located outside the focus at the time of exposure of the frame.

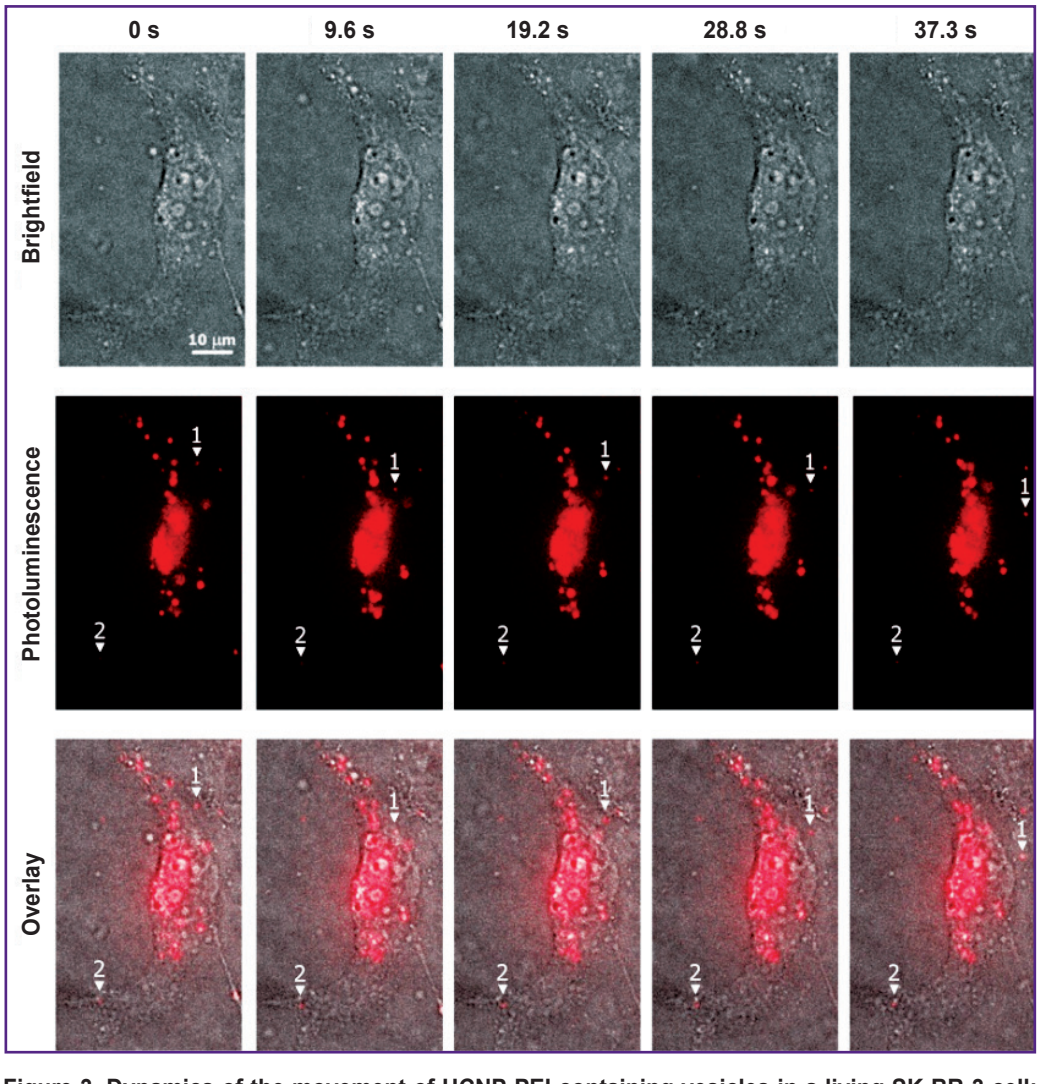

Figure 3. Dynamics of the movement of UCNP-PEI-containing vesicles in a living SK-BR-3 cell: video file shots at time points 0, 9.6, 19.2, 28.8, 37.3 s (see video)
Upper row: brightfield images; middle row: photoluminescence images of UCNP-PEI, recorded in the range of 420–842 nm; lower row: overlay images

While visually analyzing the video files obtained, we noted that some particles undergo flick and directional movements. These movements usually last for several seconds and resume after short pauses, which is typical for the intracellular transport of nanoparticles encapsulated in vesicles [19, 25]. In particular, such behavior is demonstrated by the particle marked under number *1* in Figure 3. At the same time, some of the UCNP-PEI particles perform random spatial fluctuations with relatively small amplitudes (see the particle marked under number *2* in Figure 3).

To determine the location of particles *1* and *2*, we have fitted the PL spots corresponding to these particles by the Gaussian function (1) on each frame of the time interval from 0 to 37.3 s. Figure 4 shows an example of determining the UCNP-PEI location.

The particle trajectories calculated in this way are shown in Figure 5. Particle *2* moves in a limited region with an area of less than 4 μm^2, while particle *1* is moved to more than 14 μm from its original location. The most likely mechanism for the particle *1* moving is active intracellular transport through microtubules or actin filaments [26].

Figure 6 shows the graphs of cumulative and relative displacements, depending on the time of observation of

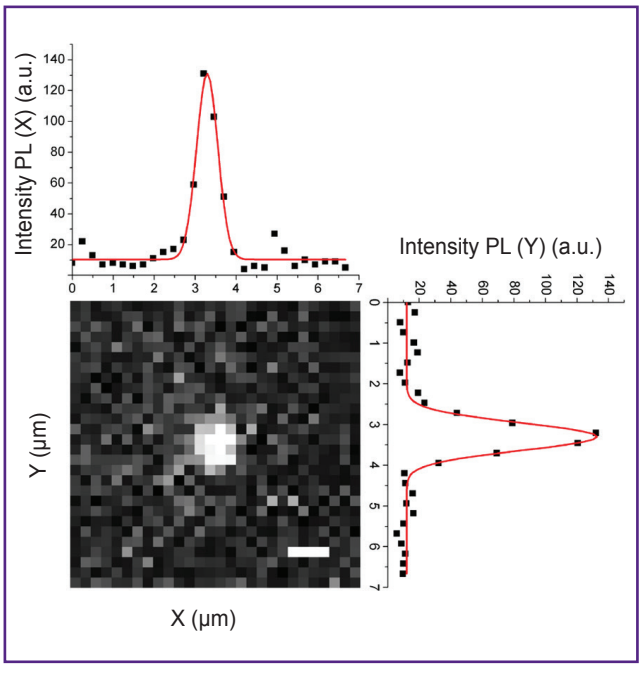

Figure 4. Determination of the location of the vesicle containing the UCNP-PEI particles by fitting by the Gaussian function. The scale bar is 1 μm

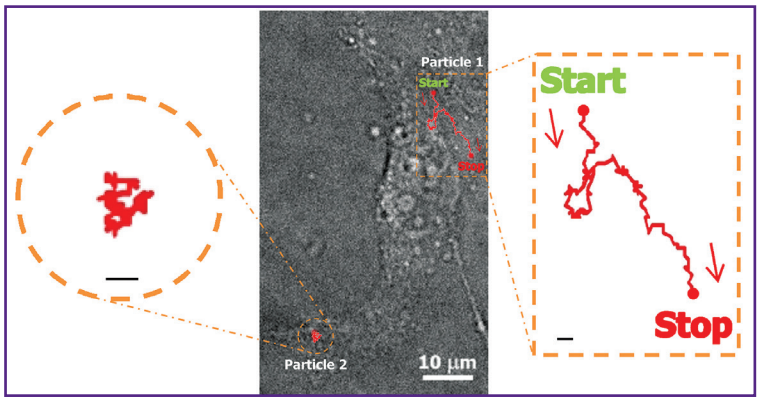

Figure 5. Trajectories of the UCNP-PEI particles *1* and *2* in SK-BR-3 cell
On the right and left inserts, the red color indicates the pathway traversed in 37.3 s by the particles *1* and *2*, respectively. The scale bar on the inserts is 1 μm

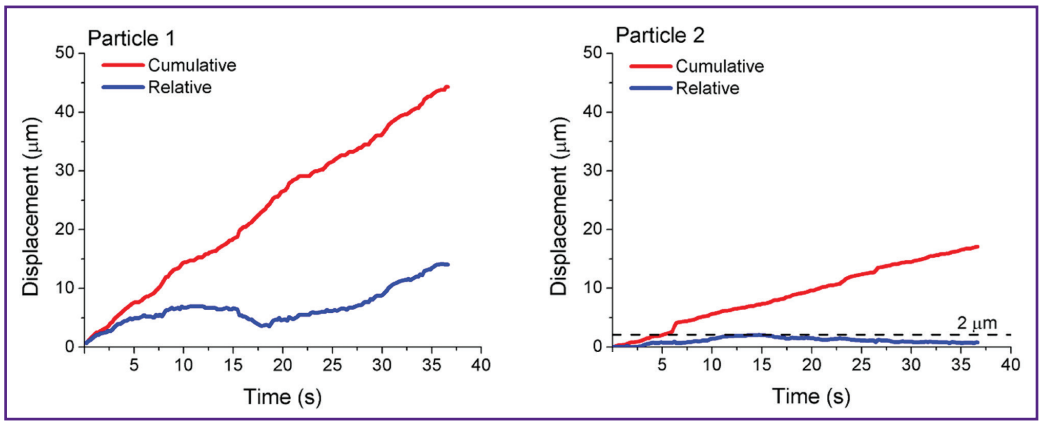

Figure 6. Cumulative and relative displacements of particles *1* and *2*, depending on the time of the observation

the UCNP-PEI particles indicated in Figure 3. The velocity of motion of the two types of particles noted above calculated on the basis of cumulative displacement differs several times (about 2.5). In order of magnitude, the particle velocities determined in our work (0.4±1.2 μm/s) agree with the data of [19], in which the tracking of UCNPs in a cell was performed.

Another indicator shown in Figure 6 is the relative displacement (*blue curves*). In the case of direction motion, the displacement reached a significant value (Figure 6 (a)), whereas for random motion the displacement did not exceed 2 μm (Figure 6 (b)).

An important aspect that must be taken into account when carrying out long-term observations of living cells is the preservation of their viability throughout the experiment. In our study, the cells remained viable for 3 h. This opens possibilities for long-term monitoring of biological processes of interest in a cancer cell.

Conclusion

In this paper, we implemented a scheme for tracking of $NaYF_4$:Yb,Tm nanoparticles coated with polyethylenimine in living cells using wide-field microscopy. The observed nonspecific tracking of UCNP-PEI in human breast adenocarcinoma cells SK-BR-3 showed that UCNPs are an advanced agent for dynamic studies of intracellular processes.

The key advantages of the proposed tracking scheme with the use of UCNP-PEI and wide-field microscopy are the almost complete absence of autofluorescence, which ensures a high selectivity of PL registration, and fast rate of image acquisition, which makes it possible to study fast intracellular processes.

Further improvement of the photophysical properties of UCNPs and the use of surface conjugation schemes will expand the use of UCNPs as a PL marker for monitoring intracellular processes.

Acknowledgments. The work was financially supported by the Ministry of Education and Science of Russia (contract No.14.Z50.31.0022).

Conflicts of interest. The authors declare that there are no conflicts of interest regarding the publication of this paper.

References

1. Kusumi A., Tsunoyama T.A., Hirosawa K.M., Kasai R.S., Fujiwara T.K. Tracking single molecules at work in living cells. *Nat Chem Biol* 2014; 10(7): 524–532, https://doi.org/10.1038/nchembio.1558.

2. Pinaud F., Clarke S., Sittner A., Dahan M. Probing cellular events, one quantum dot at a time. *Nat Methods* 2010; 7(4): 275–285, https://doi.org/10.1038/nmeth.1444.

3. Gerion D., Pinaud F., Williams S.C., Parak W.J., Zanchet D., Weiss S., Alivisatos A.P. Synthesis and properties of biocompatible water-soluble silica-coated CdSe/ZnS semiconductor quantum dots. *J Phys Chem B* 2001; 105(37): 8861–8871, https://doi.org/10.1021/jp0105488.

4. Parak W.J., Boudreau R., Le Gros M., Gerion D., Zanchet D., Micheel C.M., Williams S.C., Alivisatos A.P., Larabell C. Cell motility and metastatic potential studies based on quantum dot imaging of phagokinetic tracks. *Adv Mater* 2002; 14(12): 882–885, https://doi.org/10.1002/1521-4095(20020618)14:12<882::aid-adma882>3.0.co;2-y.

5. Dahan M., Levi S., Luccardini C., Rostaing P., Riveau B., Triller A. Diffusion dynamics of glycine receptors revealed by single-quantum dot tracking. *Science* 2003; 302(5644): 442–445, https://doi.org/10.1126/science.1088525.

6. Lidke D.S., Nagy P., Heintzmann R., Arndt-Jovin D.J., Post J.N., Grecco H.E., Jares-Erijman E.A., Jovin T.M. Quantum dot ligands provide new insights into erbB/HER receptor-mediated signal transduction. *Nat Biotechnol* 2004; 22(2): 198–203, https://doi.org/10.1038/nbt929.

7. Yao J., Larson D.R., Vishwasrao H.D., Zipfel W.R., Webb W.W. Blinking and nonradiant dark fraction of water-soluble quantum dots in aqueous solution. *Proc Natl Acad Sci USA* 2005; 102(40): 14284–14289, https://doi.org/10.1073/pnas.0506523102.

8. Nirmal M., Dabbousi B.O., Bawendi M.G., Macklin J.J., Trautman J.K., Harris T.D., Brus L.E. Fluorescence intermittency in single cadmium selenide nanocrystals. *Nature* 1996; 383(6603): 802–804, https://doi.org/10.1038/383802a0.

9. Chen N., He Y., Su Y.Y., Li X.M., Huang Q., Wang H.F., Zhang X.Z., Tai R.Z., Fan C.H. The cytotoxicity of cadmium-based quantum dots. *Biomaterials* 2012; 33(5): 1238–1244, https://doi.org/10.1016/j.biomaterials.2011.10.070.

10. Zvyagin A.V., Sreenivasan V.K.A., Goldys E.M., Panchenko V.Y., Deyev S.M. Photoluminescent hybrid inorganic-protein nanostructures for imaging and sensing in vivo and in vitro. *Smart Materials Series* 2015; p. 245–284, https://doi.org/10.1039/9781782622109-00245.

11. Generalova A.N., Rocheva V.V., Nechaev A.V., Khochenkov D.A., Sholina N.V., Semchishen A., Zubov V.P., Koroleva A.V., Chichkov B.N., Khaydukov E.V. PEG-modified upconversion nanoparticles for in vivo optical imaging of tumors. *RSC Advances* 2016; 6(36): 30089–30097, https://doi.org/10.1039/c5ra25304g.

12. Deng M.L., Ma Y.X., Huang S., Hu G.F., Wang L.Y. Monodisperse upconversion $NaYF_4$ nanocrystals: syntheses and bioapplications. *Nano Research* 2011; 4(7): 685–694, https://doi.org/10.1007/s12274-011-0124-y.

13. Park Y.I., Kim J.H., Lee K.T., Jeon K.-S., Na H.B., Yu J.H., Kim H.M., Lee N., Choi S.H., Baik S.I., Kim H., Park S.P., Park B.J., Kim Y.W., Lee S.H., Yoon S.Y., Song I.C., Moon W.K., Suh Y.D., Hyeon T. Nonblinking and nonbleaching upconverting nanoparticles as an optical imaging nanoprobe and T1 magnetic resonance imaging contrast agent. *Adv Mater* 2009; 21(44): 4467–4471, https://doi.org/10.1002/adma.200901356.

14. Guller A.E., Generalova A.N., Petersen E.V., Nechaev A.V., Trusova I.A., Landyshev N.N., Nadort A., Grebenik E.A., Deyev S.M., Shekhter A.B., Zvyagin A.V. Cytotoxicity and non-specific cellular uptake of bare and surface-modified upconversion nanoparticles in human skin cells. *Nano Research* 2015; 8(5): 1546–1562, https://doi.org/10.1007/s12274-014-0641-6.

15. Vedunova M.V., Mishchenko T.A., Mitroshina E.V., Ponomareva N.V., Yudintsev A.V., Generalova A.N., Deyev S.M., Mukhina I.V., Semyanov A.V., Zvyagin A.V. Cytotoxic effects of upconversion nanoparticles in primary

hippocampal cultures. *RSC Advances* 2016; 6(40): 33656–33665, https://doi.org/10.1039/c6ra01272h.

16. Grebenik E.A., Kostyuk A.B., Deyev S.M. Upconversion nanoparticles and their hybrid assemblies for biomedical applications. *Russian Chemical Reviews* 2016; 85(12): 1277–1296, https://doi.org/10.1070/rcr4663.

17. Sreenivasan V.K.A., Zvyagin A.V., Goldys E.M. Luminescent nanoparticles and their applications in the life sciences. *J Phys Condens Matter* 2013; 25(19): 194101, https://doi.org/10.1088/0953-8984/25/19/194101.

18. Bonnet J., Burton J., Kardos K., Vail T., Niedbala R.S., Tanke H.J. Detection of cell and tissue surface antigens using up-converting phosphors: a new reporter technology. *Anal Biochem* 1999; 267(1): 30–36, https://doi.org/10.1006/abio.1998.2965.

19. Nam S.H., Bae Y.M., Park Y.I., Kim J.H., Kim H.M., Choi J.S., Lee K.T., Hyeon T., Suh Y.D. Long-term real-time tracking of lanthanide ion doped upconverting nanoparticles in living cells. *Angew Chem Int Ed Engl* 2011; 50(27): 6093–6097, https://doi.org/10.1002/ange.201007979.

20. Jo H.L., Song Y.H., Park J., Jo E.-J., Goh Y., Shin K., Kim M.-G., Lee K.T. Fast and background-free three-dimensional (3D) live-cell imaging with lanthanide-doped upconverting nanoparticles. *Nanoscale* 2015; 7(46): 19397–19402, https://doi.org/10.1039/c5nr05875a.

21. Zhao J.B., Jin D.Y., Schartner E.P., Lu Y.Q., Liu Y.J., Zvyagin A.V., Zhang L.X., Dawes J.M., Xi P., Piper J.A., Goldys E.M., Monro T.M. Single-nanocrystal sensitivity achieved by enhanced upconversion luminescence. *Nat Nanotechnol* 2013; 8(10): 729–734, https://doi.org/10.1038/nnano.2013.171.

22. Michalet X. Mean square displacement analysis of single-particle trajectories with localization error: Brownian motion in an isotropic medium. *Physical Review E* 2010; 82(4): 041914, https://doi.org/10.1103/physreve.82.041914.

23. Ma N.N., Ma C., Li C.Y., Wang T., Tang Y.J., Wang H.Y., Mou X.B., Chen Z., He N.Y. Influence of nanoparticle shape, size, and surface functionalization on cellular uptake. *J Nanosci Nanotechnol* 2013; 13(10): 6485–6498, https://doi.org/10.1166/jnn.2013.7525.

24. Conner S.D., Schmid S.L. Regulated portals of entry into the cell. *Nature* 2003; 422(6927): 37–44, https://doi.org/10.1038/nature01451.

25. Wen L., Zheng Z.H., Liu A.A., Lv C., Zhang L.J., Ao J., Zhang Z.L., Wang H.Z., Lin Y., Pang D.W. Tracking single baculovirus retrograde transportation in host cell via quantum dot-labeling of virus internal component. *J Nanobiotechnology* 2017; 15(1): 37, https://doi.org/10.1186/s12951-017-0270-9.

26. Alberts B., Johnson A., Lewis J., Raff M., Roberts K., Walter P. *Molecular biology of the cell.* New York: Garland Science; 2008.